Received: 6 May 2018 | Revised: 21 January 2019 | Accepted: 31 January 2019

DOI: 10.1002/ima.22313

WILEY

RESEARCH ARTICLE

Comparative evaluation of the polynomial and spline fitting methods for the B0 correction of CEST MRI data acquired from human brains

Chang Hyun Yoo[1] | Janghoon Oh[2] | Soonchan Park[3] | Chang-Woo Ryu[3] | Young Kyun Kwon[1] | Geon-Ho Jahng[3]

[1]Department of Physics and Research Institute for Basic Sciences, Kyung Hee University, Seoul, Republic of Korea

[2]Department of Radiology, Kyung Hee University Hospital, Kyung Hee University, Seoul, Republic of Korea

[3]Department of Radiology, Kyung Hee University Hospital at Gangdong, College of Medicine, Kyung Hee University, Seoul, Republic of Korea

Correspondence
Geon-Ho Jahng, Department of Radiology, Kyung Hee University Hospital at Gangdong, College of Medicine, Kyung Hee University, 892 Dongnam-ro, Gangdong-Gu, Seoul 05278 Republic of Korea.
Email: ghjahng@gmail.com

Funding information
Convergence of Conventional Medicine and Traditional Korean Medicine R&D program funded by the Ministry of Health & Welfare through the Korea Health Industry Development Institute, Grant/Award Number: HI16C2352; National Research Foundation of Korea grant funded by the Korea government, Grant/Award Number: 2014R1A2A2A01002728

Abstract

To compare the magnetization transfer ratio asymmetry (MTR_{asym}) values calculated with polynomial and spline fitting methods for B0 correction of the full Z-spectrum images, full Z-spectrum data was obtained from 12 elderly healthy subjects by using a 3D segmented EPI sequence, as well as from 17 other subjects by using a 3D GRASE sequence with two different 3 T MRI systems. The full Z-spectra were analyzed to map MTR_{asym} with three different fitting methods, namely the 10th and 14th polynomial and spline methods, for B0 correction. The MTR_{asym} values for each offset frequency were compared among the three fitting methods. For the 3D segmented EPI sequence, the MTR_{asym} values significantly differed among the three fitting methods at 0.86, 2.14, 3.00, and 3.43 ppm offset frequencies. For the 3D GRASE sequence, the MTRasym values obtained by 14th polynomial and spline fitting methods significantly differed at arbitrary offset frequencies. The MTR_{asym} values are sensitive to the fitting methods of B0 correction and to the type of acquisition sequence for the full Z-spectrum. Therefore, an appropriate fitting method should be used to analyze the full Z-spectrum obtained from the brain.

KEYWORDS

full Z-spectrum, MTR asymmetry, polynomial fitting, sequence type, spline fitting

1 | INTRODUCTION

Chemical exchange saturation transfer (CEST) MRI enables molecules or proteins to be imaged by receiving a signal from selectively saturated protons without exposure or chemical compound injection.[1,2] These frequency-dependent saturation effects are visualized as a signal loss at a specific frequency, known as a Z-spectrum[3] or CEST spectrum. In the CEST imaging technique, images are acquired by applying a saturation radiofrequency (RF) pulse with different offset frequencies. The saturation effects are asymmetric with respect to the water resonance frequency. A CEST asymmetric map is typically used to evaluate CEST effects by asymmetry analysis where the water signal from one side of the Z-spectrum is subtracted from the signal from the other side. The CEST technique was used to map exchangeable protons, including amide (–NH), amine ($–NH_2$), guanidino ($[NH_2]_2$), and hydroxyl (–OH) groups within phantoms, animals, and the human body.[4] Furthermore, the CEST technique has been used for the imaging of various brain diseases, including strokes, tumors, multiple sclerosis,[5] and Alzheimer's disease.[6]

In the homogenous magnetic field, the full Z-spectrum indicates the lowest signal at the center of the water frequency. However, a frequency shift may occur owing to the inhomogeneity of the magnetic field; therefore, the frequency of the lowest signal is shifted upstream or downstream from

the center of the water frequency. To correctly calculate the asymmetry of the magnetization transfer ratio (MTR) from the full Z-spectrum data, the frequency shift must be fixed before mapping the MTR asymmetry (MTR_{asym}). Several fitting methods, such as the polynomial[7,8] or spline[2,9,10] methods, have been used to find the water frequency. The fitting process, which is called a B0 correction, is one of the critical components of analyzing the full Z-spectrum MRI data because the frequency shift is directly related to mapping MTR_{asym}. For a CEST experiment, the CEST effect is usually demonstrated by calculating the MTR asymmetry by estimating the signal difference between two different frequency offsets, which represents the asymmetry of the full Z spectrum. Therefore, the MTR asymmetry indicates a quantitative estimation of the saturation transfer phenomenon caused by the saturation pulse. In this study, we also calculated MTR asymmetry values at a certain frequency offset to demonstrate the saturation transfer effect.

Although a previous phantom study evaluated the full Z-spectrum data with the spline and polynomial methods,[9] no systematic study has been performed to compare MTR_{asym} with different fitting methods for the B0 correction of the full Z-spectrum data obtained from the human brain. The objective of this study was, therefore, to compare MTR_{asym} values in the amide, amine, guanidine, and hydroxyl offset frequencies calculated using three different fitting methods (10th and 14th polynomial and spline method) applied to the full Z-spectrum data acquired from two different CEST MRI sequences in the human brain.

2 | MATERIALS AND METHODS

2.1 | Subjects

This study was approved by the ethical committee of our Institutional Review Board. Twenty-nine healthy elderly subjects were studied using two different sequences. In the first group, 12 subjects (2 men and 10 women; age = 73.83 ± 8.92 y; range = 55-83 y) were scanned with a three-dimensional (3D) segmented gradient-echo echo-planar imaging (EPI) sequence to obtain full Z-spectrum signals by using a 3 T MRI system (Achieva 3.0 T, Philips Medical System, Best, the Netherlands). In the second group, 17 subjects (4 men and 13 women; age = 71.7 ± 11.48 y; range = 38-92 y) were scanned with a 3D gradient- and spin-echo (GRASE) sequence to obtain full Z-spectrum signals by using another 3 T MRI system (Ingenia 3.0 T, Philips Medical System, Best, the Netherlands). All subjects were recruited for the optimization of the CEST MRI technique in our institute's hospital.

2.2 | MRI acquisition

The first full Z-spectrum data was acquired with the 3D segmented gradient-echo EPI sequence[11] from the brain by using an eight-channel sensitivity-encoding (SENSE) coil. To induce the saturation transfer of protons, we utilized the following parameters: the B_1 amplitude of the saturation pulse = 1 μT; the saturation pulse duration per pulse = 70 ms; and the total number of shots to the center of the *k*-space = 126. Therefore, the total saturation length was 8.8 seconds. We obtained the full Z-spectrum via 29 dynamics from offset frequencies in the range of −6.00 to 6.00 ppm by using the continuously increased frequency interval of 0.42 or 0.43 ppm. The first acquired image was the reference image S_0 at −40 ppm offset frequency. The imaging parameters were as follows: repetition time (TR)/echo time (TE) = 150/7.1 ms; acquisition matrix = 112 × 112; acquisition voxel size = 2 × 2 × 6.40 mm^3; reconstruction voxel size = 0.76 × 0.76 × 3.20 mm^3; EPI factor = 9; flip angle (FA) = 7°; field-of-view (FOV) = 220 × 220 × 106 mm^3; SENSE factor = 2 for the anterior-posterior direction and 1 for the right-left direction; number of slices = 33; and imaging orientation = transverse. The scan time was 9 minutes 27 seconds.

The second full Z-spectrum data was acquired with the 3D GRASE sequence[12] from the brain by using a 32 channel SENSE coil. To induce CEST saturation exchange, we used the following parameters: the B_1 amplitude = 2 μT; the saturation pulse duration = 200 ms with a pulse interval = 10 ms; and the number of saturation pulses = 4. Therefore, the total saturation length was 0.84 seconds. We obtained the full Z-spectrum via 37 dynamics from offset frequencies in the range of −5.00 to 5.00 ppm by using an alternative increased frequency interval of 0.25 ppm from offset frequencies ranging from ±0.25 to ±4.00 ppm, and thereafter offset frequencies of ±4.5 and ±5.0 ppm. The first acquired image was the reference image S_0 at an offset of −40 ppm and the second acquired image was at an offset of 0 ppm with respect to the direct saturation of water. The imaging parameters were: TR/TE =2200/16 ms; acquisition matrix = 104 × 92; acquisition voxel size = 2 × 2 × 8 mm^3; reconstruction matrix size = 1 × 1 × 4 mm^3; FA = 90°; SENSE factor = 2 for the anterior-posterior direction and 1 for the right-left direction; turbo spin-echo (TSE) factor = 23; EPI factor = 7; number of slices = 23; and imaging orientation = transverse. The scan time was 8 minutes 29 seconds.

Finally, for image registration and brain tissue segmentation, sagittal structural 3D T1-weighted (3D T1W) images were acquired by the magnetization-prepared rapid acquisition of gradient echo sequence with the following parameters: TR = 8.1 ms; TE = 3.7 ms; FA = 8°; FOV = 236 × 236 mm^2; and voxel size = 1 × 1 × 1 mm^3. In addition, T2-weighted TSE and fluid-attenuated inversion recovery images were acquired to examine any brain malformations.

2.3 | Fitting the full Z-spectrum data by three different methods to map MTR asymmetry

All the MRI data was handled using MATLAB (http://www.mathworks.com) (Mathworks, Natick, Massachusetts) to map

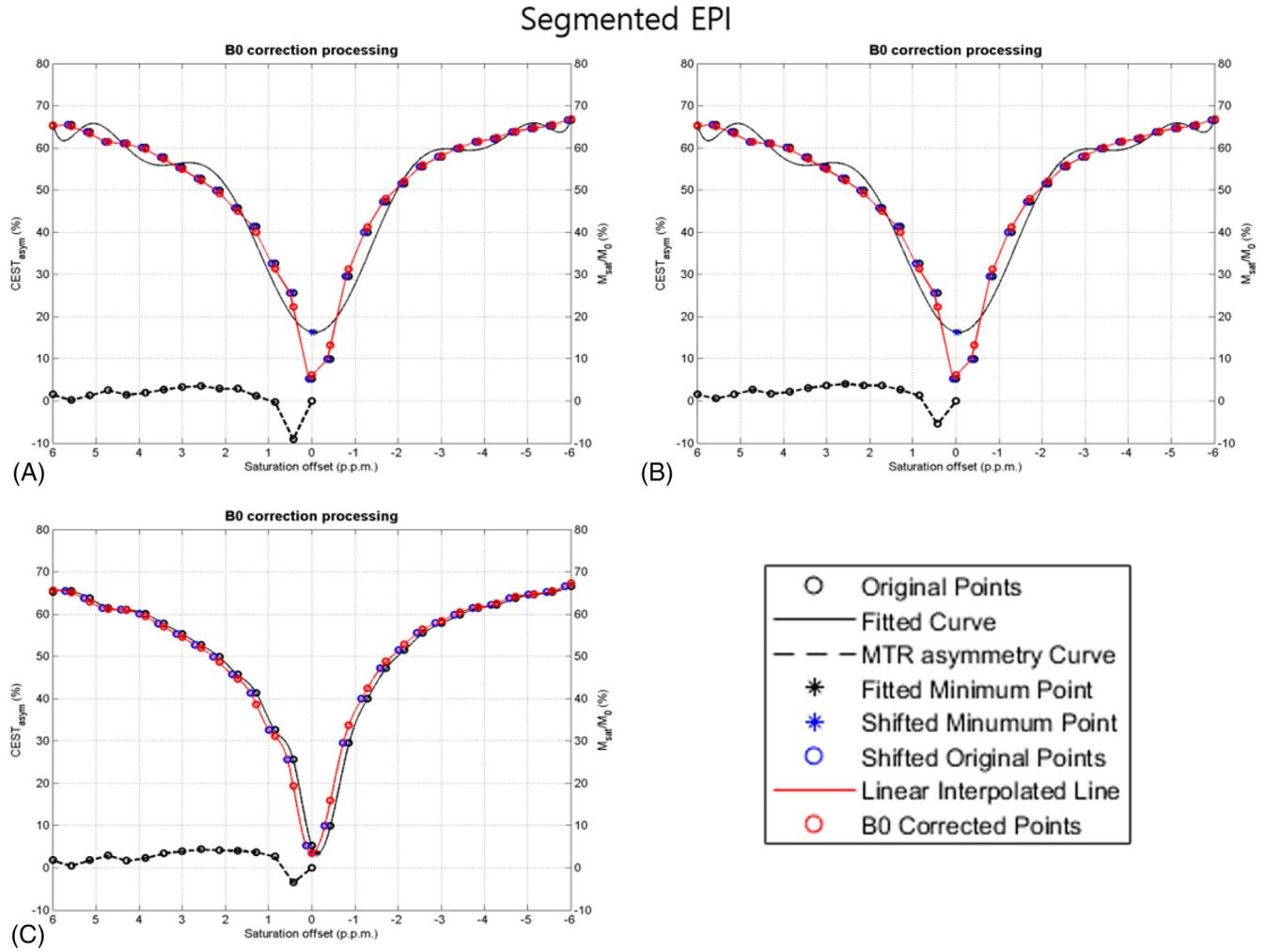

FIGURE 1 Full Z-spectrum (Figure 1-A, 1-B, 1-C) acquired with the 3D segmented echo-planar imaging sequence from one subject in the left precuneus region and the corresponding MTR_{asym} map (Figure 1-D, 1-E, 1-F) calculated with three different fitting methods, the 10th (Figure 1-A) and 14th (Figure 1-B) order polynomial fitting and spline (Figure 1-C) fitting. In Figure 1-A, 1-B, 1-C, the black solid line indicates the fitting curve, the red solid line indicates the B0 corrected curve, and the black dotted line indicates the MTR_{asym} curve. In Figure 1-D, 1-E, 1-F, the maps show MTR_{asym} obtained from four different frequency offsets with the corresponding reference imaging (Ref). The bright color indicates a higher MTR_{asym} value [Color figure can be viewed at wileyonlinelibrary.com]

the voxel-based MTR_{asym} from the full Z-spectrum data. First, the nonbrain tissue was removed by using brain extraction tool (BET) masking[13] to extract the Z-spectrum data from the brain alone. Second, the full Z-spectrum images were divided by the reference image S_0 obtained at −40 ppm offset frequency. Third, the voxel-based B0 correction was performed by three different fitting methods, namely, the 10th and 14th polynomial[14] and spline[10] methods. For the polynomial fitting method, the following equation was used with $n = 10$ and 14 for the 10th and 14th polynomial fittings, respectively: $f(x) = \sum_{k=0}^{n} a_k x^k = a_n x^n + a_{n-1} x^{n-1} + \ldots + a_2 x^2 + a_1 x^1 + a_0$. The water resonance frequency was estimated as the frequency with the lowest signal intensity from the fitted curve and shifted along the direction of the offset axis to 0 ppm at its lowest intensity. Finally, the MTR_{asym} map for each fitting method was calculated by using the following equation[14,15]:

$$MTR_{asym} = \frac{S_{sat}(-\Delta\omega) - S_{sat}(+\Delta\omega)}{S_0}$$

where S_{sat} $(\pm\Delta\omega)$ are the signals obtained at $\pm\Delta\omega$ offset frequencies and S_0 is the signal obtained at an offset frequency of −40 ppm. For the 3D segmented EPI data, the MTR_{asym} maps for the three fitting methods were selected at saturation offsets of 0.86 ppm (hydroxyl), 2.14 ppm (guanidino), 3.00 ppm (amine), and 3.43 ppm (amide). For the 3D GRASE data, the MTR_{asym} maps for the three fitting methods were selected at saturation offsets of 1.00 ppm (hydroxyl), 2.00 ppm (guanidino), 3.00 ppm (amine), and 3.50 ppm (amide).

2.4 | Postprocessing of the MTR_{asym} map

Before comparing the MTR_{asym} maps among the three fitting methods for each sequence, we performed the following steps using the Statistical Parametric Mapping version 12 (SPM12) software (http://www.fil.ion.ucl.ac.uk/spm/software/spm12/). First, the 3D T1W image and the reference image S_0 for each subject were co-registered. Subsequently, all MTR_{asym} maps were also co-registered to the 3D T1W image. Second, the 3D

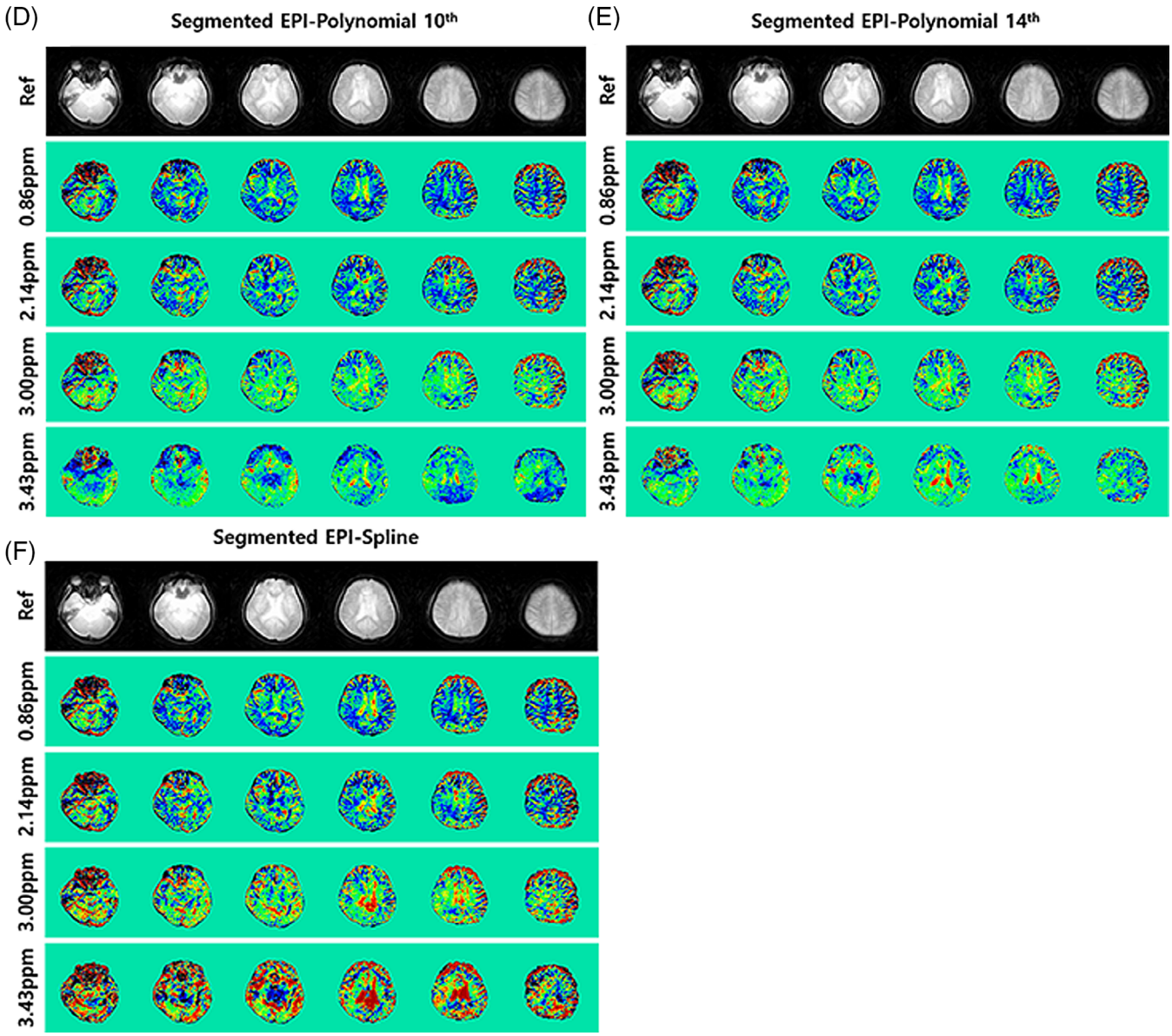

FIGURE 1 (Continued)

T1W image was segmented into gray matter and white matter using the CAT12 toolbox (http://www.neuro.uni-jena.de/cat/) to obtain brain tissue compartments and to spatially normalize the segmented tissue map to the standard Montreal Neurological Institute template. The corresponding MTR_{asym} maps were also normalized into the template using the deformation field information of the 3D T1W image. Finally, all MTR_{asym} maps were smoothed with the full-width half maximum of the $8 \times 8 \times 8$ mm^3 Gaussian smoothing kernel for voxel-based statistical analysis.

2.5 | Statistical analyses of the MTR_{asym} map

Statistical analyses were performed with both voxel-based and region-of-interest (ROI)-based methods. For the voxel-based analysis, the paired *t* test was performed to compare the MTR_{asym} values obtained from the three fitting methods and subsequently repeated three times for each specific offset frequency for each sequence. A significance level of 0.0001 was applied without correction for multiple comparison and clusters with at least 30 contiguous voxels. The results of voxel-wise analyses were also used to define ROI in the brain.

For the ROI-based analysis, ROI areas that demonstrated significant levels from the voxel-based analyses were defined using the WFU_Pickatlas toolbox (http://fmri.wfubmc.edu/software/PickAtlas). We selected the left and right cuneus, insula, and precuneus for the 3D-segmented EPI sequence and at the left and right caudate body, parahippocampal gyrus, and precuneus for the 3D GRASE sequence. MTR_{asym} values were extracted from the selected ROIs using the Marsbar toolbox (http://marsbar.sourceforge.net). As the MTR_{asym} values were not normally distributed by the Kolmgorov-Smirnov method,[16] the Wilcoxon rank sum test[17] was used to evaluate the difference in the MTR_{asym} values among the three fitting methods

TABLE 1 Results of ROI-based analyses of MTR_{asym} values for each offset frequency obtained from the 3D segmented EPI sequence after polynomial (poly) and spline fittings of the full Z-spectrum

Cuneus_LT	PPM	Poly10	Poly14	Spline	*P*-value
SEG-EPI		Median (95%CI)	Median (95%CI)	Median (95%CI)	A/B/C
	3.43	−7.75 (−15.0950 - −2.8876)	−7.755 (−13.5920 - −0.3766)	−3.285 (−10.5842 - 2.3154)	0.0522/0.0024/0.0049
	3.00	−3.505 (−9.2220 - 5.5083)	−3.045 (−8.2219 - 1.9762)	−1.455 (−5.8836 - 6.4149)	0.0640/0.0640/0.0771
	2.14	−0.02 (−2.4868 - 6.6906)	2.545 (0.1456 - 6.9410)	6.795 (4.3283 - 12.5407)	0.0771/0.0093/0.0010
	0.86	−1.5 (−7.6556 - 3.8415)	2.47 (0.6585 - 5.2982)	10.215 (2.5932 - 17.7654)	0.0923/0.0122/0.0156
Cuneus_RT	**PPM**	**Poly10**	**Poly14**	**Spline**	***P*-value**
SEG-EPI		**Median (95%CI)**	**Median (95%CI)**	**Median (95%CI)**	**A/B/C**
	3.43	−11.985 (−22.4391 - −1.3467)	−12.33 (−21.8179 - −2.2757)	−8.37 (−19.2346 - 4.7074)	0.0923/0.0269/0.0342
	3.00	−9.935 (−14.9553 - 5.4343)	−9.125 (−12.9415 - 5.8033)	−4.31 (−12.8387 - 7.7524)	0.0923/0.0161/0.1763
	2.14	0.52 (−6.1202 - 7.4650)	1.33 (−4.6750 - 5.5950)	3.715 (−0.6687 - 13.3372)	0.1294/0.0342/0.0034
	0.86	1.59 (−7.9599 - 5.3260)	3.06 (0.1136 - 5.0682)	17.5 (6.9480 - 21.7587)	0.0923/0.0161/0.0068
Insula_LT	**PPM**	**Poly10**	**Poly14**	**Spline**	***P*-value**
SEG-EPI		**Median (95%CI)**	**Median (95%CI)**	**Median (95%CI)**	**A/B/C**
	3.43	−7.65 (−11.7467 - −6.1942)	−7.13 (−11.9727 - −5.4827)	−6.415 (−9.5759 - −2.7551)	0.1099/0.0210/0.0161
	3.00	4.635 (−10.5278 - −0.6144)	−4.845 (−11.1639 - 0.6263)	−1.46 (−7.9862 - 1.8343)	0.0522/0.0161/0.0210
	2.14	2.615 (0.6189 - 5.7977)	3.56 (0.3535 - 7.0283)	6.72 (1.9122 - 12.4214)	0.1475/0.0522/0.0640
	0.86	5.305 (0.002575 - 7.2175)	6.575 (3.8284 - 10.1372)	18.645 (3.9024 - 32.0867)	0.0771/0.0210/0.0522
Insula_RT	**PPM**	**Poly10**	**Poly14**	**Spline**	***P*-value**
SEG-EPI		**Median (95%CI)**	**Median (95%CI)**	**Median (95%CI)**	**A/B/C**
	3.43	−7.285 (−17.9482 - −2.8744)	−6.535 (−16.8782 - −2.7103)	−5.53 (−17.4424 - 0.9910)	0.0010/0.0210/0.0923
	3.00	−10.05 (−17.1006 - −0.008134)	−9.175 (−15.4327 - 1.0471)	−7.14 (−17.1790 - 5.5132)	0.0034/0.0522/0.2334
	2.14	1.635 (−1.7262 - 8.3999)	2.91 (−3.2951 - 8.5206)	3.83 (−0.5008 - 14.1634)	0.0210/0.0640/0.1763
	0.86	−0.955 (−4.3317 - 4.5898)	4.275 (−0.09832 - 11.1378)	14.495 (2.5439 - 33.5943)	0.0024/0.0122/0.0522
Precuneus_LT	**PPM**	**Poly10**	**Poly14**	**Spline**	***P*-value**
SEG-EPI		**Median (95%CI)**	**Median (95%CI)**	**Median (95%CI)**	**A/B/C**
	3.43	−4.865 (−16.6477 - −0.9556)	−2.62 (−15.4603 - 0.01921)	−1.135 (−15.3042 - 5.8750)	0.0015/0.0122/0.1099
	3.00	−1.09 (−5.9594 - 3.0228)	0.97 (−3.8081 - 6.7588)	3.585 (−2.8753 - 11.5595)	0.0015/0.0015/0.0093
	2.14	2.425 (−0.7410 - 16.2065)	8.305 (3.8176 - 18.1952)	15.59 (6.3898 - 18.6073)	0.0015/0.0010/0.0161
	0.86	−8.815 (−15.5289 - 0.4922)	1.315 (−1.4304 - 6.3551)	14.355 (1.1624 - 24.2148)	0.0010/0.0024/0.0342
Precuneus_RT	**PPM**	**Poly10**	**Poly14**	**Spline**	***P*-value**
SEG-EPI		**Median (95%CI)**	**Median (95%CI)**	**Median (95%CI)**	**A/B/C**
	3.43	−8 (−17.0691 - 2.2122)	−7.655 (−16.0257 - 3.8266)	−5.14 (−16.1822 - 6.6940)	0.0342/0.0122/0.0923
	3.00	−6.335 (−7.8562 - 3.5571)	−4.96 (−7.5498 - 6.2587)	−0.99 (−3.4079 - 7.7284)	0.0156/0.0010/0.0024
	2.14	0.385 (−3.9127 - 13.8721)	4.775 (−0.6021 - 15.9248)	8.895 (1.6465 - 13.8068)	0.0049/0.0161/0.1099
	0.86	−8.455 (−14.1373 - 1.8330)	−0.73 (−2.5689 - 7.4037)	10.47 (−7.9801 - 19.8414)	0.0034/0.0210/0.1514

Data shows median, 95% confidential interval (CI), and p-value.
The P-values were obtained by the Wilcoxon rank sum test between the polynomials of 10th and 14th orders (A), between the polynomial of 10th order and the spline (B), and between the polynomial of 14th order and the spline (C).

for each ROI, each offset frequency, and each sequence. A *P*-value of less than 0.0167 (0.05/3) was used to determine the significance level because we repeated the paired-wise comparisons three times for each frequency offset for each sequence. The statistical evaluation was performed using the Medcalc statistical program (http://www.medcalc.org).

3 | RESULTS

Figure 1 shows the full Z-spectrum (Figure 1-A, 1-B, 1-C) acquired with the 3D-segmented EPI sequence from one subject and the corresponding MTR_{asym} map (Figure 1-D, 1-E, 1-F) calculated using three different fitting methods, 10th and 14th polynomial fitting and spline fitting, in the left precuneus region. The fitting results are slightly different between the polynomial and spline fitting methods (Figure 1-A, 1-B, 1-C). The results between the two polynomial fittings are similar, but the MTR_{asym} line under the fitted curve shows the difference between the two polynomial fittings (Figure 1-A, 1-B). MTR_{asym} values obtained using spline fitting are slightly higher than those obtained using polynomial fittings (Figure 1-D,1-E,1-F), as listed in Tables 1 and 2.

TABLE 2 Results of ROI-based analyses of MTR_{asym} values for each offset frequency obtained from 3D GRASE sequence after polynomial (poly) and spline fittings of the full Z-spectrum

Caudate_Body_LT	PPM	Poly10	Poly14	Spline	*P*-value
GRASE		Median (95%CI)	Median (95%CI)	Median (95%CI)	A/B/C
	3.50	−9.64 (−36.5635-7.7179)	−15.25 (−47.8662-10.2153)	18.02 (2.5234-41.4467)	0.1743/0.0569/0.0505
	3.00	1.08 (−15.1039-11.7434)	−5.6 (−31.0659-9.0687)	23.58 (2.3602-51.2025)	0.1743/0.0569/0.0714
	2.00	2.52 (−6.0287-5.5211)	0.88 (−26.8657-4.4765)	26.58 (8.3353-52.0712)	0.1743/0.0174/0.0202
	1.00	−2.33 (−6.6044-0.2805)	−1.74 (−5.4637-8.1503)	36.56 (14.4238-49.6400)	0.0887/0.0004/0.0007
Caudate_Body_RT	**PPM**	**Poly10**	**Poly14**	**Spline**	***P*-value**
GRASE		**Median (95%CI)**	**Median (95%CI)**	**Median (95%CI)**	**A/B/C**
	3.50	−17.24 (−43.5434-−0.6982)	−24.94 (−43.0890-−1.4054)	30.42 (9.5295-44.7353)	0.3060/0.0093/0.0079
	3.00	−7.44 (−24.1573-4.2441)	−11.01 (−22.6244-5.1115)	40.75 (0.007601-62.9145)	0.1454/0.0026/0.0056
	2.00	−5.04 (−15.1133-5.2573)	−10.68 (−24.3566-1.3658)	71.51 (34.3800-83.9405)	0.0174/0.0026/0.0013
	1.00	−3.74 (−8.7968-1.8142)	1.13 (−7.6837-7.1526)	65.36 (36.7172-76.6644)	0.0569/0.0038/0.0038
Parahippocampal_LT	**PPM**	**Poly10**	**Poly14**	**Spline**	***P*-value**
GRASE		**Median (95%CI)**	**Median (95%CI)**	**Median (95%CI)**	**A/B/C**
	3.50	18.68 (15.3935-22.5882)	22.4 (14.5424-28.3887)	33.14 (0.7449-39.6373)	0.0638/0.4874/0.4874
	3.00	15.75 (9.9576-20.0168)	20.18 (13.7242-28.3621)	15.19 (−8.2543-28.0766)	0.1089/0.4307/0.1743
	2.00	10.34 (4.4061-20.0212)	13.36 (9.1455-27.5770)	7.78 (−14.3515-12.8698)	0.0110/0.1202/0.0348
	1.00	1.93 (−1.4736-5.0260)	4.32 (−0.4056-10.2636)	−0.11 (−14.6430-7.5794)	0.0569/0.2247/0.0569
Parahippocampal_RT	**PPM**	**Poly10**	**Poly14**	**Spline**	**P-Value**
GRASE		**Median (95%CI)**	**Median (95%CI)**	**Median (95%CI)**	**A/B/C**
	3.50	19.38 (10.5106-25.1254)	21.14 (10.9051-29.7971)	30.53 (9.0254-77.2629)	0.5791/0.3529/0.4038
	3.00	16.04 (12.5574-20.0994)	16.43 (13.3431-21.8689)	17.97 (12.1359-31.0436)	0.8176/0.3529/0.4874
	2.00	12.94 (7.9379-14.7078)	10.25 (6.8032-17.3389)	11.71 (9.2132-26.5136)	0.7119/0.3060/0.3529
	1.00	2.09 (0.04790-4.1382)	1.82 (−1.0170-4.9237)	3.64 (1.4639-13.1767)	0.7119/0.1901/0.2842
Precuneus_LT	**PPM**	**Poly10**	**Poly14**	**Spline**	***P*-value**
GRASE		**Median (95%CI)**	**Median (95%CI)**	**Median (95%CI)**	**A/B/C**
	3.50	2.2 (−7.4868-10.5752)	5.81 (−1.1861-12.5973)	9.34 (−7.8504-21.4326)	0.1743/0.7119/0.8536
	3.00	10.39 (6.8235-13.9286)	12.3 (7.5296-16.6377)	19.07 (0.3741-24.5408)	0.0348/0.6112/1.0000
	2.00	7.26 (4.0611-10.7260)	9.51 (8.0427-15.7726)	17.59 (8.9343-24.2968)	0.2247/0.2633/0.5791
	1.00	0.28 (−2.1697-2.9168)	2.57 (0.7052-5.1913)	6.2 (2.1150-15.3860)	0.1324/0.0348/0.2247
Precuneus_RT	**PPM**	**Poly10**	**Poly14**	**Spline**	***P*-value**
GRASE		**Median (95%CI)**	**Median (95%CI)**	**Median (95%CI)**	**A/B/C**
	3.50	6.54 (−0.3966-10.8337)	8.03 (1.8624-11.8226)	9.43 (−34.3271-18.7010)	0.4038/0.4307/0.6777
	3.00	12.86 (9.4234-15.1768)	13.78 (8.4923-18.2187)	19.53 (−7.7358-28.9118)	0.1901/0.8900/0.6441
	2.00	8.06 (5.7039-10.6939)	11.95 (7.0913-15.5215)	13.28 (0.8012-24.7639)	0.5477/0.4874/0.7819
	1.00	0.08 (−2.3687-2.3000)	0.98 (0.2584-3.2849)	8.79 (−0.09001-11.3371)	0.3778/0.0505/0.2247

Data shows median, 95% confidential interval (CI) and *P*-value.
The *P*-values were obtained by the Wilcoxon rank sum test between the polynomials of 10th and 14th orders (A), between the polynomial of 10th order and the spline (B), and between the polynomial of 14th order and the spline (C).

Figure 2 shows the full Z-spectrum (Figure 2-A, 2-B, 2-C) acquired with the 3D GRASE sequence from another subject and the corresponding MTR_{asym} map (Figure 2-D, 2-E, 2-F) calculated using three different fitting methods, 10th and 14th polynomial fittings and spline fitting, in the left precuneus region. The full Z-spectrum acquired with the 3D GRASE sequence is much broader than that acquired with the 3D-segmented EPI sequence. The overall MTR_{asym} maps with the 3D GRASE sequence are poorer than those with the 3D-segmented EPI sequence (Figure 2-D, 2-E, 2-F). The fitting results are slightly different between the polynomial and spline fitting methods (Figure 2-A, 2-B, 2-C). It is unclear as to which fitting method is better.

3.1 | Voxel-based analysis

The results of voxel-based comparison of the MTR_{asym} maps among the three fitting methods are shown in Figure 3 for the 3D-segmented EPI sequence and in Figure 4 for the 3D GRASE sequence. The detailed areas, which show significant difference among the three fitting methods, are listed in Supporting Information Table S1 for the 3D-segmented EPI sequence and in Supporting Information Table S2 for the 3D GRASE sequence. The MTR_{asym} values are significantly

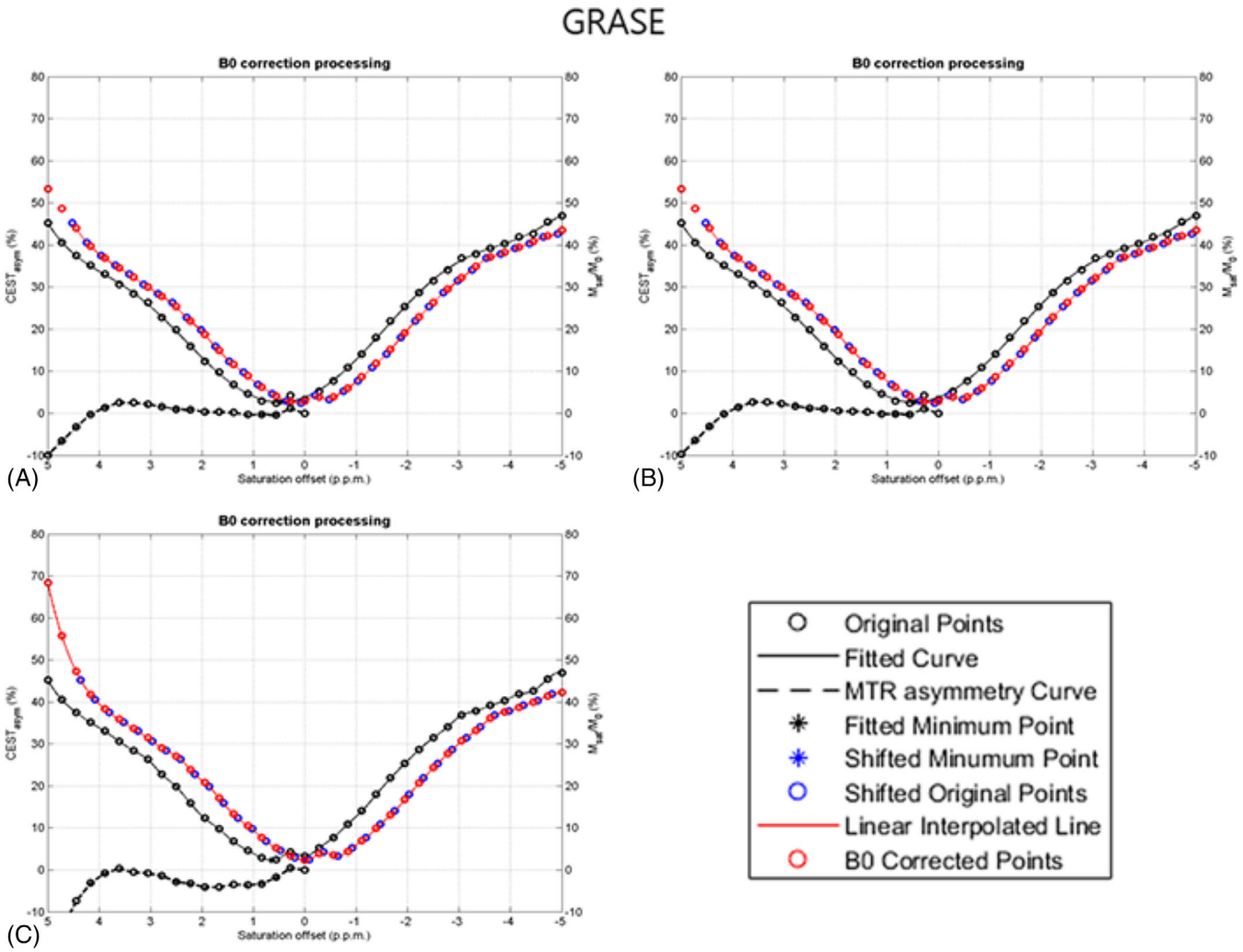

FIGURE 2 Full Z-spectrum (Figure 2-A, 2-B, 2-C) acquired with the 3D GRASE sequence from one subject in the left precuneus region and the corresponding MTR_{asym} map (Figure 2-D, 2-E, 2-F) calculated with three different fitting methods, the 10th (Figure 2-A) and 14th (Figure 2-B) order polynomial fitting and spline (Figure 2-C) fitting. In Figure (2-A, 2-B, 2-C), the black solid line represents the fitting curve, the red solid line indicates the B0 corrected curve, and the black dotted line indicates the MTR_{asym} curve. In Figure (2-D, 2-E, 2-F), the maps show MTR_{asym} obtained from four different frequency offsets with the corresponding reference imaging (Ref). The bright color indicates a higher MTR_{asym} value [Color figure can be viewed at wileyonlinelibrary.com]

different between the three fitting methods at the 3.00 ppm. and 3.43 ppm. saturation offset frequencies for the 3D-segmented EPI sequence (Figure 3) and at the 3.0 ppm. and 3.5 ppm. saturation offset frequencies for the 3D GRASE sequence. In addition, the MTR_{asym} values are not significantly different among the three fitting methods at the 0.86 ppm. saturation offset frequency for the 3D-segmented EPI sequence (Supporting Information Figure S1) but are significantly different among the three fitting methods at a 1.00 ppm. saturation offset frequency for the 3D GRASE sequence (Supporting Information Figure S2). Finally, the MTR_{asym} values are significantly different among the three fitting methods at a 2.14 ppm. saturation offset frequency for the 3D-segmented EPI sequence (Supporting Information Figure S1) and at a 2.00 ppm. saturation offset frequency for the 3D GRASE sequence (Supporting Information Figure S2). The detailed areas that showed significant differences among the three fitting methods were listed in Supporting Information Table S3 for the 3D-segmented EPI sequence and in Supporting Information Table S4 for the 3D GRASE sequence.

3.2 | ROI-based analysis

The results of ROI-based comparison of the MTR_{asym} values among the three fitting methods for each ROI and for each offset frequency are listed in Table 1 for the 3D-segmented EPI sequence and in Table 2 for the 3D GRASE sequence. For the segmented-EPI sequence (Table 1), the MTR_{asym} values between the 10th and 14th polynomial fitting orders are not significantly different for both the left and right cuneus' and the left insular for the four offset frequencies but are significantly different in the right insula for the offset frequencies, except at 2.14 ppm. The MTR_{asym} values between the spline fitting and polynomial fitting methods are not significantly different in the left cuneus at a 3.00 ppm. offset, the right cuneus at a 3.43 ppm. offset, and the right insular at

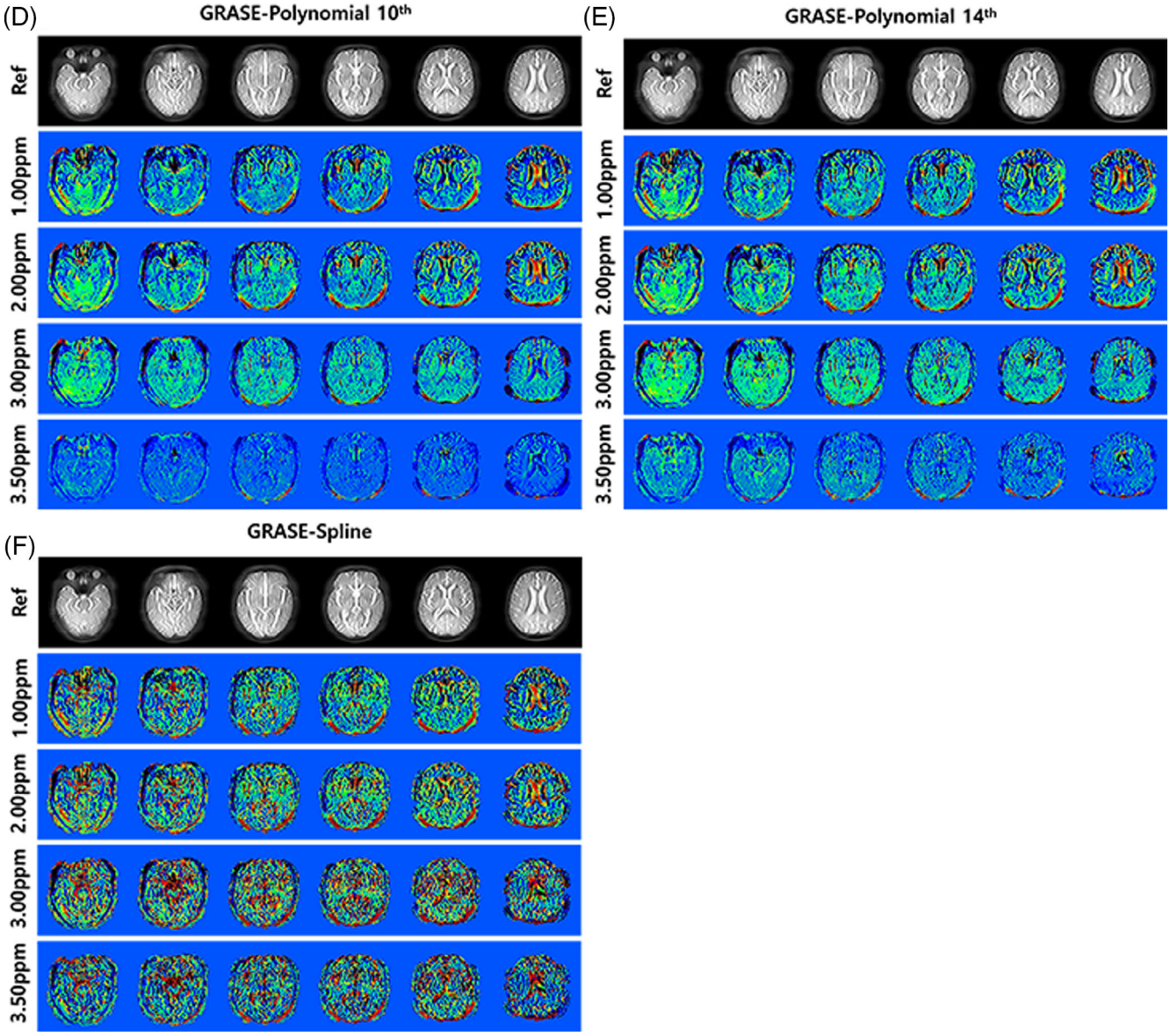

FIGURE 2 (Continued)

3.00 ppm. and 3.43 ppm. offset frequencies but are significantly different elsewhere. The MTR_{asym} values between the 10th and 14th polynomial fitting orders are significantly different in both the left and right precuneus for the four offset frequencies but are not significantly different in the right precuneus at the 3.43 ppm. offset frequency. The MTR_{asym} values between the polynomial 10th and spline fitting methods are significantly different in the left and right precuneus for the four offset frequencies but are not significantly different in the right precuneus at the 0.86 ppm. offset frequency. The MTR_{asym} values between the polynomial 14th and spline fitting methods are not significantly different in both the left and right precuneus at the 3.43, 2.14, and 0.86 ppm. offset frequencies, except for the left precuneus at the 2.14 ppm. offset frequency.

With the GRASE sequence (Table 2), the MTR_{asym} values between the 10th and 14th polynomial fitting orders are not significantly different in both the left and right caudate body and the parahippocampal for the four offset frequencies but are significantly different in the left parahippocampal at the 2.00 ppm. offset frequency. The MTR_{asym} values between the spline and polynomial fitting methods are not significantly different in the left and right parahippocampal for the four offset frequencies and in the left caudate body at the 3.50, 3.00, and 2.00 ppm. offset frequencies but are significantly different elsewhere. The MTR_{asym} values among the three fitting methods are not significantly different in both the left and right precuneus for the four offset frequencies.

4 | DISCUSSION

B0 correction, which allows one to obtain the correct frequency of water, is one of the most important steps to calculate the

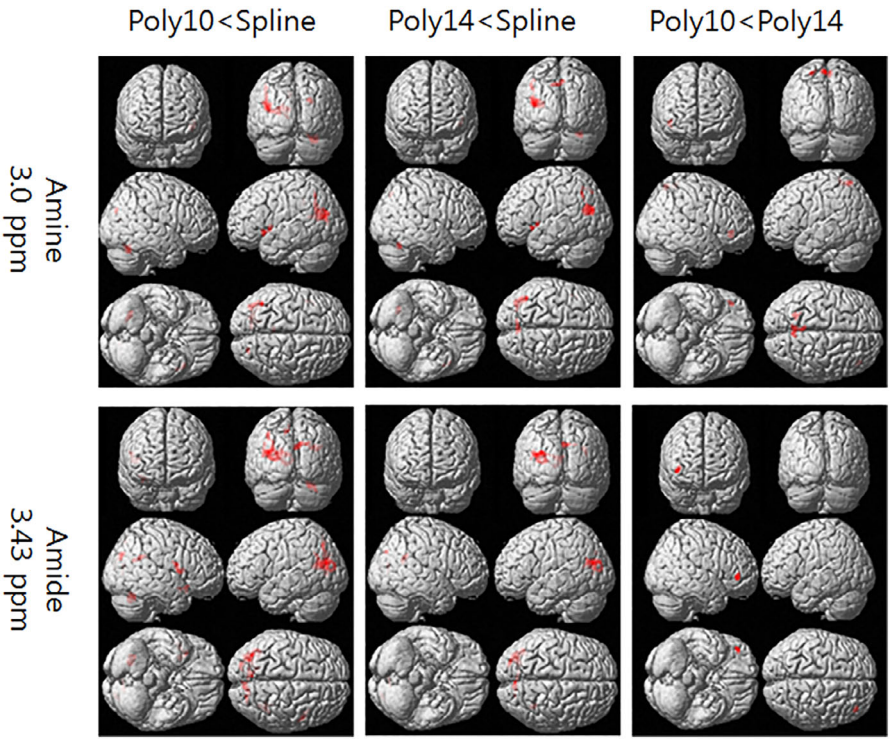

FIGURE 3 Result of the voxel-based comparisons of MTR_{asym} maps at 3.0 and 3.43 ppm offset frequencies among the three fitting methods calculated from the 3D segmented EPI data The red color indicates that MTR_{asym} values are greater than one of the other fitting methods [Color figure can be viewed at wileyonlinelibrary.com]

MTR_{asym} value from the full Z-spectrum data. Although one study performed a comparison between the polynomial and spline fitting methods in a phantom experiment, no comparative studies have yet been conducted on humans. The main purpose of this study, therefore, is to compare the MTR_{asym} values calculated from three different fitting methods with two different imaging sequences. The major findings of this study are that (a) MTR_{asym} values are different depending on the fitting

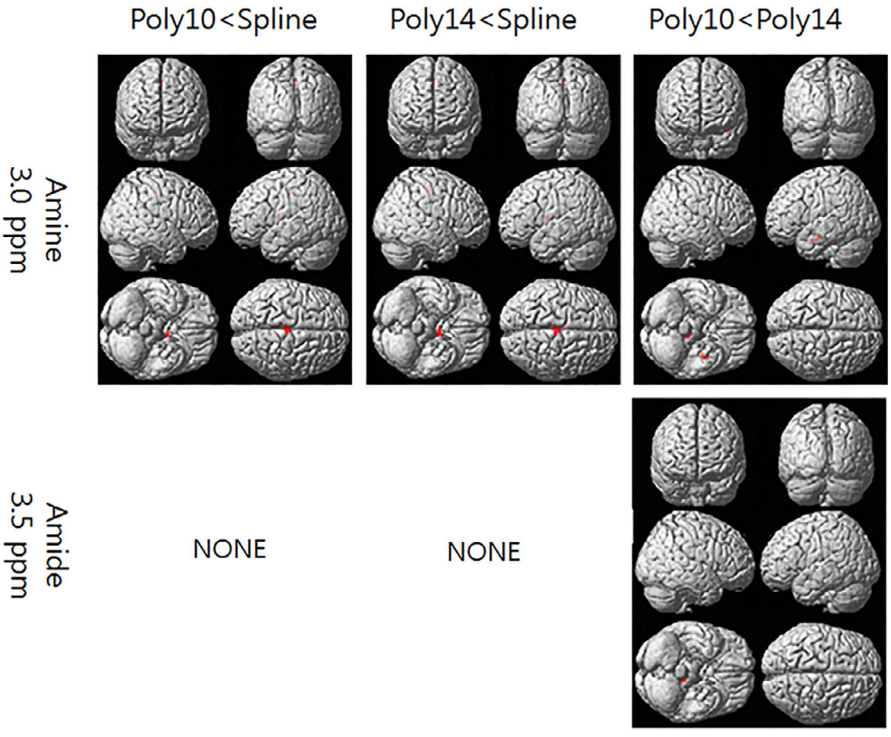

FIGURE 4 Result of the voxel-based comparisons of MTR_{asym} maps at 3.0 and 3.5 ppm offset frequencies among the three fitting methods calculated from the 3D GRASE data. The red color indicates that MTR_{asym} values are greater than one of the other fitting methods [Color figure can be viewed at wileyonlinelibrary.com]

method and (b) that MTR_{asym} values are strongly sensitive to the type of imaging sequences with the same fitting method. In this study, we used the following notations for the frequency offsets: 0.86 ppm for hydroxyl, 2.14 ppm for guanidino, 3.00 ppm for amine, and 3.43 ppm for amide protons for the 3D-segmented EPI data, and 1.00 ppm for hydroxyl, 2.00 ppm for guanidino, 3.00 ppm for amine, and 3.50 ppm for amide protons for the 3D GRASE data.

4.1 | MTR_{asym} values are different among the three fitting methods

The fitting method affects the MTR_{asym} values. The result of the ROI-based analysis demonstrated that for the EPI sequence, the MTR_{asym} values with spline fitting is different compared to that with the 10th and 14th polynomial fitting method (Figure (1-A, 1-B, 1-C)). For the GRASE sequence, the MTR_{asym} values obtained with the 10th and 14th polynomial fitting methods are similar but the results obtained with the polynomial and spline fitting methods are different (Figure (2-A, 2-B, 2-C)). The fitting results are dependent on the selected ROIs. For example, with the segmented EPI-sequence (Table 1), the MTR_{asym} values at the right insula are significantly different between the 10th and 14th polynomial fitting orders but are not significantly different between the 14th polynomial fitting and spline fitting methods. With the GRASE sequence (Table 2), the MTR_{asym} values in the right caudate body are significantly different between the polynomial fitting and spline fitting methods but are not significantly different between the 10th and 14th polynomial fitting orders. It is observed that the fitting results depend on the fitting methods on the selected ROIs.

The main difference between the spline and polynomial fitting methods is whether they divide a fitting section. The spline fitting method divides the data into sections and connects data by fitting them to a low order polynomial. The polynomial fitting method fits the entire data to a high-order polynomial at once. A previous study[9] showed differences between the spline and polynomial methods in a phantom experiment with suspensions at different liposome concentrations, which had a relatively homogeneous magnetic field compared to the human brain. The polynomial fitting method seemed to fit the data well when a high order is used, but the fitting lines were quite different between when using polynomials of the 12th and 24th orders.[9] Near 0 ppm, the 24th polynomial method fitted the data better than the 12th polynomial method. After 5 ppm, Runge's wiggles did not fit well for both the 12th and 24th orders. The polynomial-fitted curve was well matched to the original point near 0 ppm when the order was high. To analyze the full Z spectrum, researchers have used higher degree polynomials such as the 12th order polynomial rather than a lower degree polynomial. In this study, we also used a higher degree polynomial because a lower degree polynomial does not fit well near the direct water saturation (DWS) frequency offset, which is 0 ppm at the full Z spectrum. Instead, the lower degree polynomial fits the data better than the higher degree polynomial at a frequency offset farther away from 0 ppm because the Runge's wiggle phenomenon is observed under the same condition. Typically, a lower degree polynomial is not required because the full Z spectrum is usually acquired within ±6 ppm in most CEST experiments. A higher degree polynomial that fits well around 0 ppm is more useful. Thus, this study used 10th and 14th order polynomials similar to 12th order polynomial.

4.2 | Fitting results are dependent on the type of the imaging sequences

MTR_{asym} values of the same fitting method vary depending on the type of imaging pulse sequences. The result of the ROI-based analysis shows that in the segmented-EPI sequence (Table 1), MTR_{asym} values between the polynomial 10th and 14th fitting methods are significantly different both in the left and right precuneus at four offset frequencies, except at 3.43 ppm in the right precuneus. However, in the GRASE sequence (Table 2), MTR_{asym} values among the three fitting methods are not significantly different in the left and right percuneus for four offset frequencies. This may be related to the sensitivity to the B0 inhomogeneity of the EPI sequence. For the GRASE sequence, several spin-echo pulses are generally used to reverse spins, which are less sensitive to field inhomogeneity. Therefore, the fitting result is better with the GRASE sequence than with the EPI sequence. The broad Z-spectrum with the GRASE sequence may be another cause of insensitivity to the choice of the fitting method. Therefore, for the CEST experiment in the brain, it is important to choose a proper sequence to minimize the fitting error.

4.3 | Limitation

This study has certain limitations. First, the polynomial fittings were evaluated for the 10th and 14th order. Compared with the difference between 12th and 24th orders,[9] 10th and 14th orders may be too close to determine the difference of the fitting results. In a future study, comparative evaluations of more orders are planned to be performed. Second, our results may not confirm which fitting method is the best to use in evaluating the full Z-spectrum obtained from the human brain because there is no gold standard method. Therefore, a researcher needs to apply fitting methods in a trial-and-error manner. Finally, the number of subjects in each sequence was relatively small. Therefore, it would be necessary to carry out additional studies using more subjects.

5 | CONCLUSION

We found that MTR_{asym} values are dependent on the fitting methods and very sensitive to the type of the imaging sequences when the same fitting method is used. Although

the 3D GRASE sequence has a much broader Z-spectrum than that acquired with the 3D segmented EPI sequence, MTR_{asym} values with the 3D GRASE sequence are less sensitive to the fitting method than those with the 3D segmented EPI sequence. Therefore, it is necessary to select the fitting method according to the sequence to obtain an effective CEST effect in the brain.

ACKNOWLEDGMENTS

This study was supported by the National Research Foundation of Korea (NRF) grant funded by the Korean government (MSIP) (2014R1A2A2A01002728) and the Convergence of Conventional Medicine and Traditional Korean Medicine R&D program funded by the Ministry of Health & Welfare through the Korea Health Industry Development Institute (KHIDI) (HI16C2352).

CONFLICT OF INTEREST

The authors declare that they have no conflict of interest.

ORCID

Geon-Ho Jahng https://orcid.org/0000-0001-8881-1884

REFERENCES

1. Dagher AP, Aletras A, Choyke P, Balaban RS. Imaging of urea using chemical exchange-dependent saturation transfer at 1.5T. *J Magn Reson Imaging*. 2000;12(5):745-748.
2. Oh J-H, Kim H-G, Woo D-C, Jeong H-K, Lee SY, Jahng G-H. Chemical-exchange-saturation-transfer magnetic resonance imaging to map gamma-aminobutyric acid, glutamate, myoinositol, glycine, and asparagine: phantom experiments. *J Korean Phys Soc*. 2017;70(5):545-553.
3. Bryant RG. The dynamics of water-protein interactions. *Annu Rev Biophys Biomol Struct*. 1996;25:29-53.
4. Ward KM, Aletras AH, Balaban RS. A new class of contrast agents for MRI based on proton chemical exchange dependent saturation transfer (CEST). *J Magn Reson*. 2000;143(1):79-87.
5. Kim J, Wu Y, Guo Y, Zheng H, Sun PZ. A review of optimization and quantification techniques for chemical exchange saturation transfer MRI toward sensitive in vivo imaging. *Contrast Media Mol Imaging*. 2015;10(3):163-178.
6. Wang R, Li SY, Chen M, et al. Amide proton transfer magnetic resonance imaging of Alzheimer's disease at 3.0 Tesla: a preliminary study. *Chin Med J (Engl)*. 2015;128(5):615-619.
7. Zhou J, Blakeley JO, Hua J, et al. Practical data acquisition method for human brain tumor amide proton transfer (APT) imaging. *Magn Reson Med*. 2008;60(4):842-849.
8. Zhou J, Payen J-F, Wilson D, Traystman R, van Zijl PCM. Using the amide proton signals of intracellular proteins and peptides to detect pH effects in MRI. *Nat Med*. 2003;9(8):1085-1090.
9. Stancanello J, Terreno E, Castelli DD, Cabella C, Uggeri F, Aime S. Development and validation of a smoothing-splines-based correction method for improving the analysis of CEST-MR images. *Contrast Media Mol Imaging*. 2008;3(4):136-149.
10. Cai K, Singh A, Roalf DR, et al. Mapping glutamate in subcortical brain structures using high-resolution GluCEST MRI. *NMR Biomed*. 2013;26(10):1278-1284.
11. Sun PZ, Lu J, Wu Y, Xiao G, Wu R. Evaluation of the dependence of CEST-EPI measurement on repetition time, RF irradiation duty cycle and imaging flip angle for enhanced pH sensitivity. *Phys Med Biol*. 2013;58(17):N229-N240.
12. Zhu H, Jones CK, van Zijl PC, Barker PB, Zhou J. Fast 3D chemical exchange saturation transfer (CEST) imaging of the human brain. *Magn Reson Med*. 2010;64(3):638-644.
13. Smith SM. Fast robust automated brain extraction. *Hum Brain Mapp*. 2002;17(3):143-155.
14. Zhao X, Wen Z, Huang F, et al. Saturation power dependence of amide proton transfer image contrasts in human brain tumors and strokes at 3 T. *Magn Reson Med*. 2011;66(4):1033-1041.
15. Jahng G-H, Oh J-H. Physical Modeling of Chemical Exchange Saturation Transfer Imaging. *Prog Med Phys*. 2017;28(4):135-143.
16. Nguyen CD, Carlin JB, Lee KJ. Diagnosing problems with imputation models using the Kolmogorov-Smirnov test: a simulation study. *BMC Med Res Methodol*. 2013;13:144.
17. Natarajan S, Lipsitz SR, Fitzmaurice GM, et al. An extension of the Wilcoxon Rank-Sum test for complex sample survey data. *J R Stat Soc Ser C Appl Stat*. 2012;61(4):653-664.

SUPPORTING INFORMATION

Additional supporting information may be found online in the Supporting Information section at the end of this article.

How to cite this article: Yoo CH, Oh J, Park S, Ryu C-W, Kwon YK, Jahng G-H. Comparative evaluation of the polynomial and spline fitting methods for the B0 correction of CEST MRI data acquired from human brains. *Int J Imaging Syst Technol*. 2019;29:272–282. https://doi.org/10.1002/ima.22313